BIOCHEMISTRY

 Volume 44, Number 18 May 10, 2005

New Concepts

Trapping of Metalloradical Intermediates of the S-States at Liquid Helium Temperatures. Overview of the Phenomenology and Mechanistic Implications

Vasili Petrouleas,* Dionysios Koulougliotis, and Nikolaos Ioannidis

Institute of Materials Science, NCSR "Demokritos", 15310 Aghia Paraskevi Attikis, Greece

Received February 21, 2005; Revised Manuscript Received April 4, 2005

ABSTRACT: The oxygen-evolving complex (OEC) of photosystem II (PSII) consists of a Mn cluster (believed to be tetranuclear) and a tyrosine (Tyr Z or Y_Z). During the sequential absorption of four photons by PSII, the OEC undergoes four oxidative transitions, S_0 to S_1, ..., S_3 to $(S_4)S_0$. Oxygen evolves during the S_3 to S_0 transition (S_4 being a transient state). Trapping of intermediates of the S-state transitions, particularly those involving the tyrosyl radical, has been a goal of ultimate importance, as that can test critically models employing a role of Tyr Z in proton (in addition to electron) transfer, and also provide important clues about the mechanism of water oxidation. Until very recently, however, critical experimental information was lacking. We review and evaluate recent observations on the trapping of metalloradical intermediates of the S-state transitions, at liquid helium temperatures. These transients are assigned to Tyr $Z^{\bullet}$ magnetically interacting with the Mn cluster. Besides the importance of trapping intermediates of this unique catalytic mechanism, liquid helium temperatures offer the additional advantage that proton motions (unlike electron transfer) are blocked except perhaps across strong hydrogen bonds. This paper summarizes the recent observations and discusses the constraints that the phenomenology imposes.

The oxidation of water to molecular oxygen in green plants, algae, and cyanobacteria is catalyzed by photosystem II (PSII), a membrane−protein complex. Upon photon excitation of P_{680}, a specialized chlorophyll moiety, electron transfer to a terminal electron acceptor, an iron−quinone complex, is initiated. A Mn cluster donates an electron to P_{680}^{+} via a redox active tyrosine denoted Tyr Z or Y_Z. The Mn cluster (believed to be tetranuclear) and Tyr Z comprise what is called the oxygen-evolving complex (OEC). The OEC undergoes four oxidative state transitions [S_0 to S_1, ..., S_3 to $(S_4)S_0$] during the absorption of four photons. One electron and on the average one proton are extracted from bound water for each photon absorbed by PSII. Oxygen evolves during the S_3 to S_0 transition, the S_4 being a transient state (see refs *1* and *2* for recent reviews).

The pathway and kinetics of electron transfer in PSII are fairly well established (*3*). It is also established now, on the basis of EPR and EXAFS studies, that the oxidizing equivalents (positive holes) during the S-state transitions are stored on the Mn cluster. Water, the ultimate electron donor, must accordingly be bound in the immediate vicinity of Mn. The mechanism of proton abstraction from water is, however, debated. An elegant model that received considerable attention proposes a metalloradical mechanism for the generation of oxygen. In this model, Tyr Z abstracts hydrogen atoms from water bound to Mn (*4*). Until very recently, however,

* To whom correspondence should be addressed. E-mail: vpetr@ims.demokritos.gr. Fax: 30-210-6519430. Telephone: 30-210-6503344.

[1] Abbreviations: vis, visible light; NIR, near-IR light. The S_n state of the Mn cluster is schematically represented as $H_{4-n}[Mn]^n$, where n denotes the number of electrons abstracted from Mn and H_{4-n} the number of substrate protons remaining in the system.

10.1021/bi0503201 CCC: $30.25
Published on Web 04/16/2005

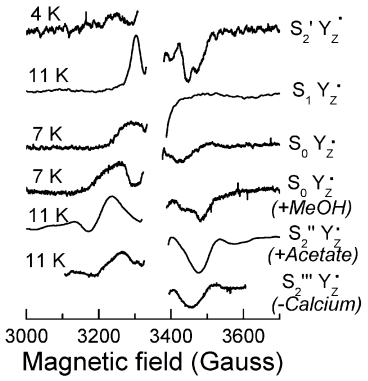

FIGURE 1: Representative spectra of the intermediates of the S-states in the intact system (top four traces), compared with the $S_2Y_Z^•$ spectra of preparations inhibited in the S_2 to S_3 step by addition of acetate or depletion of calcium (two bottom spectra). Primes distinguish different configurations of S_2. Two $S_0Y_Z^•$ spectra are shown, obtained in the absence or presence of 3% (v/v) methanol. EPR conditions: modulation amplitude of 25 G (4 G for the spectrum of $S_2'Y_Z^•$) and microwave power of 32 mW.

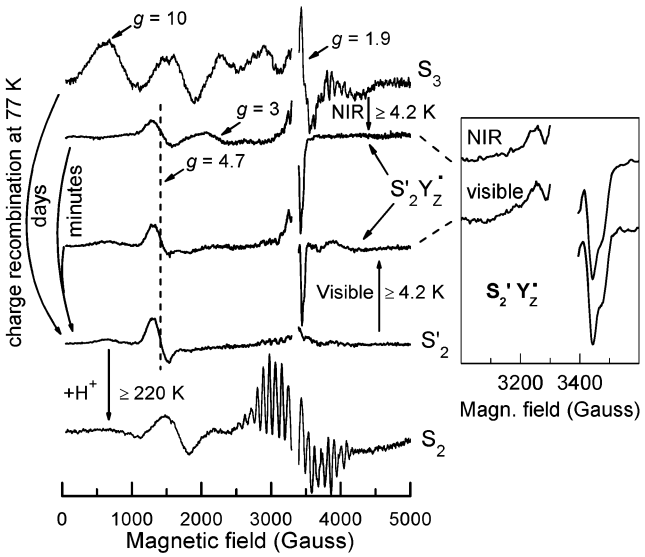

FIGURE 2: Two pathways for the formation of the $S_2'Y_Z^•$ intermediate. The inset shows an expanded view comparing the radical region of the $S_2'Y_Z^•$ spectra produced via the two different pathways.

critical experimental information was lacking. It has been thought that $Y_Z^•$ is too short-lived (or nonoxidizable at cryogenic temperatures) in intact preparations to be trapped for EPR studies. A growing body of evidence in recent years points, however, to the possibility of trapping this radical at liquid helium temperatures. Actually, intermediates of almost all S-state transitions (except the S_3 to S_0 transition) have been trapped and identified by EPR. Besides the importance of trapping intermediates of this unique catalytic mechanism, liquid helium temperatures offer the additional advantage that proton motions (unlike electron transfer) are blocked except perhaps across strong hydrogen bonds. This paper summarizes the recent observations and discusses the constraints that the phenomenology imposes.

Overview of the Experimental Observations

Examination and Assignment of the S-State Intermediates. The S-state intermediates can be induced at liquid helium temperatures either by visible-light illumination of the lower S states or by near-IR excitation of the higher S-states (*5*−*10*). Representative EPR traces emphasizing the main spectral features are shown in Figure 1 (top four traces). The spectra, taking into consideration their width, the high microwave power for saturation, and the progressive narrowing of the width at high temperatures (G. Sioros and V. Petrouleas, unpublished results), are indicative of a radical species weakly interacting with a paramagnetic metal center. These metalloradical intermediates have been assigned to Tyr Z• magnetically interacting with the Mn cluster, based on the following observations. (i) The transients can advance to the next S-state at elevated temperatures (this reaction has not been tested yet for the $S_0Y_Z^•$ transient) (*5*−*8*, *10*); this is compatible with the fact that Tyr Z• is the natural oxidant of the Mn cluster. (ii) The EPR signals are reminiscent of the signals obtained in preparations inhibited in the S_2 to S_3 step by acetate treatment or calcium depletion (bottom two spectra in Figure 1), attributed by most authors to an $S_2Y_Z^•$ intermediate (*11*−*13*). (iii) The approximate distance of Tyr Z from the Mn cluster, inferred from EPR studies (*11*−*13*), and more recently from the X-ray crystallographic studies (*14*−*16*), is 5.1−8 Å; the lower limit is an edge to edge distance (*16*), while the upper limit is the approximate distance of the centers of electronic density. This short distance is compatible with the observed magnetic broadening and the fast relaxation of the EPR signals, as well as the fact that the signals vary in shape with the oxidation state (and therefore the spin state) of the Mn cluster. (iv) Of the known electron donors implicated in side pathways, Chl_Z and Car are rather far from the Mn cluster (*14*−*16*), and have narrow-radical EPR spectra, independent of the presence or absence of Mn (*17*). It is reasonable, accordingly, to discuss this phenomenology in relation to the properties of Tyr Z, which is suitably placed and tuned to act as an intermediate of the S-state transitions.

Visible-Light versus NIR Illumination. Visible-light excitation of S_0 or S_1 at liquid helium temperatures produces $S_0Y_Z^•\cdots Q_A^-$ or $S_1Y_Z^•\cdots Q_A^-$, respectively [Figure 1 (*5*, *9*)]. The S_2 and S_3 states do not give rise to detectable levels of radical intermediates by visible-light illumination (*7*, *8*). However, near-IR excitation of the Mn cluster in S_2 or S_3 at liquid helium temperatures produces $S_1Y_Z^•$ (*8*) or $S_2'Y_Z^•$ (*7*), respectively. This unusual property is attributed to the photochemistry of a Mn(III) ion (*8*). The $S_1Y_Z^•$ signal exhibits EPR features similar to those of the one produced by visible-light excitation of S_1 (Figure 1). The rather complex but interesting phenomenology of $S_2'Y_Z^•$ formation (*6*, *7*) can be traced with the aid of Figure 2.

Charge recombination of the $S_3\cdots Q_A^-$ state (top spectrum in Figure 2 characterized by low-field signals and the $g = 1.9$ feature from the $Q_A^-Fe^{2+}$ acceptor complex) produces slowly (days to weeks) at 77 K the S_2' state (second spectrum from the bottom) (*6*). The spectrum of S_2' contains a characteristic $g = 4.7$ resonance attributed to an $S = {}^7/_2$ configuration of the Mn cluster (*18*). S_2' is a proton deficient S_2 configuration and converts to the normal S_2 state above 220 K (bottom spectrum), by proton uptake (see ref *6* for more details). Visible-light excitation of S_2' produces the $S_2'Y_Z^•$ intermediate (third spectrum in the panel and second spectrum in the inset; see also Figure 1). The spectrum is characterized by a Mn-centered part at $g = 4.7$ and a radical signal at $g = 2$ that is broadened by the magnetic interaction

with Mn (*18*). A similar spectrum can be alternatively produced by NIR excitation of the S_3 state (second spectrum from top and top spectrum in the inset) (*7*). The $g = 2$ regions of the two spectra appear to be identical within spectral resolution, but small differences can be observed in the Mn part at $g = 4.7$. The NIR-induced signal is somewhat broader and is accompanied by a $g \sim 3$ derivative. This has been attributed to small differences in the crystal field parameters of the Mn cluster (*18*); a plausible explanation is considered later in this paper. The $S_2'Y_Z^{\bullet}$ intermediates decay to the S_2' state by charge recombination of $Y_Z^{\bullet}$ with Q_A^-, at liquid helium temperatures, or reoxidize the Mn cluster at ≥ 77 K.

The observations given above are summarized by the following reactions, where use is made of the fact that most S-state transitions (except that from S_1 to S_2) are blocked below ~220 K (*19*):

$$S_0 \cdots Q_A \underset{\geq 4.2\ K}{\overset{Vis.}{\rightleftharpoons}} (S_0\, Y_Z^{\bullet} \cdots Q_A^-) \xrightarrow{> 220\ K} S_1 \cdots Q_A^- \qquad (1)$$

$$S_1 \cdots Q_A \underset{\geq 4.2\ K}{\overset{Vis.}{\rightleftharpoons}} (S_1\, Y_Z^{\bullet} \cdots Q_A^-) \underset{NIR\ \geq 4.2\ K}{\overset{\geq 77\ K}{\rightleftharpoons}} S_2 \cdots Q_A^- \qquad (2)$$

$$S_2 \cdots Q_A \underset{H^+, \geq 220\ K}{\overset{Vis, << 220\ K}{\rightleftharpoons}} S_2' \cdots Q_A \underset{77\ K,\ days}{\overset{Vis., \geq 4.2\ K}{\rightleftharpoons}} (S_2'\, Y_Z^{\bullet} \cdots Q_A^-) \underset{NIR, \geq 4.2\ K}{\overset{\geq 77\ K}{\rightleftharpoons}} S_3 \cdots Q_A^- \qquad (3)$$

$$S_3 \cdots Q_A \xrightarrow{Vis, << 220\ K} \qquad (4)$$

The reactions do not distinguish between the intermediates produced by NIR excitation of the Mn cluster and those produced by visible-light-induced charge separation. Besides potential spectral differences at $g = 2$, a notable difference is in the decay kinetics of the two sets of signals. The decay half-times of the $S_1Y_Z^{\bullet}$ and $S_2'Y_Z^{\bullet}$ transients at liquid helium temperatures are in the range of a few minutes when induced by visible light, and in the range of tens of minutes when induced by NIR excitation (*5*, *7*−*9*). A plausible explanation of this difference is provided in the next section.

The Intermediates Can Represent a Significant Fraction of Centers. Determination of the fraction of centers represented by the intermediates is not easy without knowing the low-lying spin states of the Mn cluster (the intensity of the signal will depend on factors such as transition probabilities, Boltzman distribution, etc.). Indirect estimates based on quantification of the fraction of Q_A^- acting as the acceptor partner of the metalloradical state suggest percentages of 40−50% for $S_1Y_Z^{\bullet}$ and $S_0Y_Z^{\bullet}$ (*20*).

Evaluation of the Results and Mechanistic Implications

An Interesting Correlation Exists between the Different Low-Temperature Photochemical Properties of S_0 and S_1 Compared with Those of S_2 and S_3 and the Postulated More Positive Charge on the Latter Set of States. Oxidation of Tyr Z at cryogenic temperatures correlates with less positive charge on the OEC.

It is widely accepted that the OEC is more positively charged in the S_2 and S_3 states than in the S_0 and S_1 states (see ref *21*, and critical discussions in refs *4* and *22*−*24*). The recent experiments indicate that oxidation of Tyr Z by P_{680}^+, at cryogenic temperatures, is possible only in the less positively charged S states or configurations of S states, that is, the S_0, S_1, and proton deficient S_2' states. On the other hand, the production of metalloradical intermediates by NIR excitation of the Mn cluster in the S_2 and S_3 states is coupled to the reduction of the Mn cluster at a temperature at which uptake of a compensating proton from the aqueous phase is restricted.

The Oxidation of Tyr Z at Cryogenic Temperatures Indicates Efficient Coupling to a Suitable Base, B. The oxidation potential of the protonated Tyr Z is prohibitively high, and its oxidation (at least by P_{680}^+) must be coupled to deprotonation (*22*). At liquid helium temperatures, proton motions are severely restricted, except perhaps across an existing hydrogen bond, which would likely be a tunneling and not an activated process. We must assume therefore that an efficient base, B, accepts the proton upon tyrosine oxidation (for an interesting discussion concerning the Tyr Z−base proton exchange, see ref *25*).

The Charge on the Mn Cluster Can Modulate the pK of Base B, and This Affects the Oxidizability of Tyr Z at Cryogenic Temperatures. The variation of the charge on the Mn cluster should in principle affect the oxidation potential of Tyr Z and to a lesser extent that of P_{680} by electrostatic interaction. Tyr Z should have a relatively increased oxidation potential in more positively charged states S_2 and S_3. This would slow the rate of oxidation of Tyr Z by P_{680}^+, but it is unlikely that it would block Tyr Z oxidation at cryogenic temperatures. It is more likely that the buildup of positive charge on the Mn cluster, or in its vicinity, lowers the p*K* of base B, affecting the strength of the hydrogen bonding with Tyr Z. This would slow the kinetics of Tyr Z oxidation at ambient temperature and impose kinetic barriers blocking Tyr Z oxidation at cryogenic temperatures (see also ref *25*). An impressive example is provided by the observation that the $t_{1/2}$ for Tyr D oxidation is reduced dramatically below an apparent pK_a of 7.6, and this correlates with the blockage of tyrosine oxidation below ~180 K (*26*).

An Elucidating Experiment, the Case of the Proton Deficient S_2 Configuration, S_2'. Tyr Z cannot be oxidized in S_2 and S_3 by visible-light excitation, at liquid helium temperatures. This suggests that B is not tuned to accept the proton of the tyrosine. However, as illustrated in Figure 2 and summarized by reaction 3, slow charge recombination of the $S_3 \cdots Q_A^-$ state at 77 K results in a deprotonated configuration, S_2' (*6*), which can perform low-temperature photochemistry similar to that of S_0 and S_1; i.e., it can form the $S_2'Y_Z^{\bullet}$ intermediate by visible-light illumination. The same intermediate can be produced by the NIR excitation of the S_3 state. No molecular reorganization or long-range proton motions are possible at these low temperatures. To understand these experiments, we must assume that the less positive charge on the Mn cluster in S_2' enhances the proton accepting ability of base B near Y_Z.

Of the Two Bases, Tyr Z and B, B Is More Efficiently Coupled to the Mn Cluster. Changes of the charge on the Mn cluster can modulate the relative basicity of B and Y_Z depending on their arrangement. The observations described above suggest that B is located closer to the Mn cluster, or is connected to it via a H-bond chain, while Tyr Z is positioned farther from the Mn cluster, i.e., $[Mn]^n \cdots B \cdots HY_Z$. Hence, an increase in the positive charge on the Mn cluster will cause a relative decrease in the p*K* of B. B is assumed

Scheme 1: S_0 to S_1 Transition

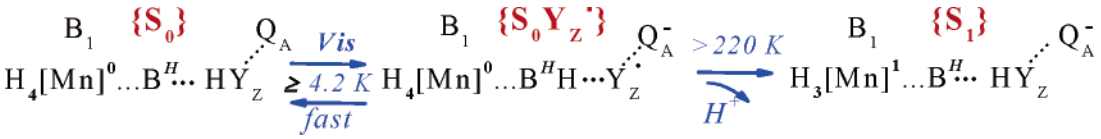

Scheme 2: S_1 to S_2 Transition[a]

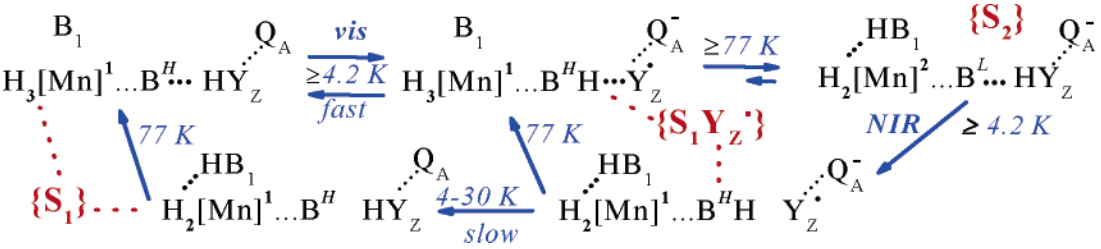

[a] The first row shows the reactions induced by visible light. There is no net proton release during this transition; instead, the proton is retained on nearby base B_1. The second row traces the reactions triggered by the NIR excitation of the S_2 state. Note the conversion of base B to a high-p*K* state, B^H, or a low-p*K* state, B^L, as the net charge on the Mn cluster changes.

Scheme 3: S_2 to S_3 Transition[a]

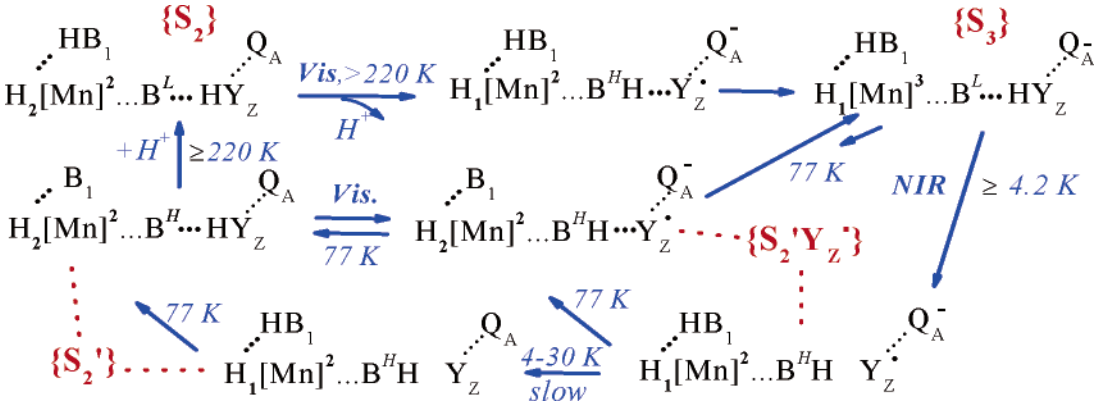

[a] All states and intermediates have been trapped and characterized by EPR, except the $S_2Y_Z^\bullet$ intermediate (middle of the first row).

to be in a high-p*K* state, B^H, in S_0, S_1, and S_2' and in a low-p*K* state, B^L, in S_2 and S_3.

The Extra Positive Charge of the S_2 and S_3 States Is Attributed to a Proton that Is Withheld during the S_1 to S_2 Transition on an Appropriate Base, B_1, in the Immediate Vicinity of the Mn Cluster. All S transitions are blocked below ~220 K (*19*), except the S_1 to S_2 transition, which can occur at temperatures close to 77 K. At 77 K, the proton released upon oxidation of the Mn cluster cannot move further than an existing H-bond; we assume that it is retained on a nearby base, denoted B_1. The more positive charge of S_2 and S_3 is attributed to it retaining this proton. The fact that the low-temperature photochemical properties of S_2 are the same whether S_2 is produced at 200 K or ambient temperature indicates that the positive charge does not move much further at equilibrium. These considerations support the suggestion that the pattern of proton release to the aqueous phase during the S_0 to S_1, ..., and S_3 to $(S_4)S_0$ transitions is close to 1, 0, 1, 2 rather than 1, 1, 1, 1 (see critical discussions in refs *4* and *22*−*24*).

Examination of the Individual S-State Transitions. A model incorporating the ideas described above is presented separately for each transition in Schemes 1−3.

S_0 to S_1 Transition (Scheme 1). This transition has a half-inhibition temperature of 220−225 K (*19*). The recent data show that illumination of S_0 readily produces $S_0Y_Z^\bullet$ down to 4.2 K (*9*, *13*). The step therefore that is blocked below 225 K must be the $S_0Y_Z^\bullet$ to S_1 transition which requires the release of a proton to the aqueous phase. The end $S_1\cdots Q_A^-$ state is unusually stable (does not decay on the tens of minutes time scale at ambient temperature; private communications with J. Messinger and I. Vass and unpublished results of N. Ioannidis and V. Petrouleas). The explanation of this behavior lies probably in the fact that the S-states recombine with Q_A^- via the metalloradical intermediates. The rate-limiting factor is the difference between the reduction potential of the various S-states and the oxidation potential of Tyr Z. The S_1/S_0 couple is known to have a redox potential at least 210 mV lower than that of the S_2/S_1 and S_3/S_2 couples (*27*).

S_1 to S_2 Transition (Scheme 2). The first line shows the charge separation reactions induced by visible light. In the last step, the Mn cluster is oxidized but the proton is retained on B_1, as described above. The increased positive charge in the vicinity converts B to a low-p*K* form, B^L. The second line shows the reactions initiated by the NIR excitation of the Mn cluster in S_2. This induces transfer of the positive hole from the Mn cluster to Tyr Z concomitant to the conversion of base B to a high-p*K* form.

S_2 to S_3 Transition (Scheme 3). This is the most complex of the three transitions but also the most informative, since the EPR signatures of all intermediates (except the interme-

Scheme 4: Proposed Reaction Model for the S_1 to S_2 Transition[a]

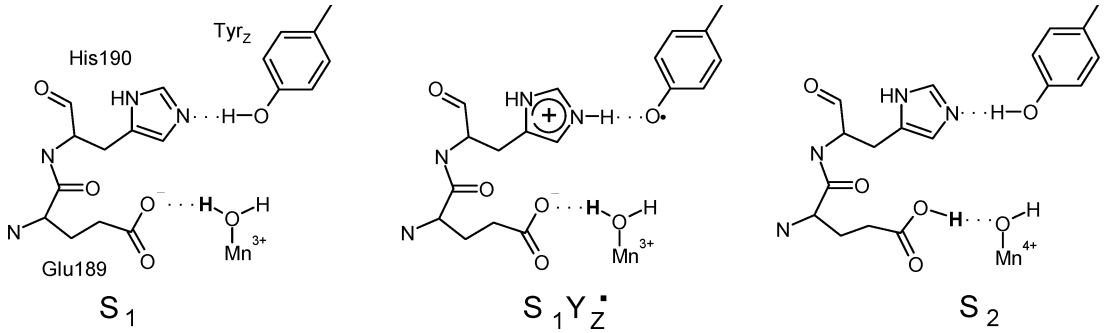

[a] Only the Mn atom close to Glu189 is shown. The water ligand of Glu189 is probably not substrate water.

diate of the S_2 to S_3 transition in the middle of first line) have been traced (Figure 2). The S_2 to S_3 transition has a half-inhibition temperature of 230 K (*19*), similar to that of the S_0 to S_1 transition, but unlike the latter, Tyr Z oxidation is not observed by visible illumination of S_2 at cryogenic temperatures. This is attributed to the low-p*K* state of B, B^L, in S_2. It is suggested in Scheme 3 (first row) that oxidation of Tyr Z is enabled by the release of a proton at high temperatures, and the concomitant conversion of base B^L to the high-p*K* form, B^H. No thermal barrier is indicated for the subsequent oxidation of the Mn cluster by Tyr Z•, but it is likely that internal charge rearrangement or bond length changes may be blocked at liquid helium temperatures (see also below). The second and third rows depict the NIR and visible-light-induced transitions between S_3 and S_2'. The reactions are entirely analogous to those between the S_1 and S_2 states (Scheme 2).

Additional Comments. It might be argued that once B is converted to low p*K* a separate base acts as the proton acceptor for Tyr Z. The inability, however, to oxidize Tyr Z by visible-light excitation of the S_2 state at cryogenic temperatures indicates that such an unconstrained coupling to a base does not exist. On the other hand, B converts readily to high p*K* even at cryogenic temperatures, once the charge on the Mn cluster changes. In Scheme 3, we adopt a concerted mechanism where oxidation of Tyr Z is coupled to the release of a proton from the Mn cluster. Presumably, a similar situation applies in the S_3 to S_4 transition.

It is assumed in Schemes 2 and 3 that the Mn cluster is reduced by NIR excitation, but the compensating proton charge stays on B_1 at low temperatures. This can explain certain observations. (i) The Mn-centered part of the NIR-induced $S_2'Y_Z$• signal ($g = 3-5$ region of Figure 2) appears to be somewhat distorted, and (ii) the recombination reaction of Y_Z• with Q_A^- at liquid helium temperatures is very slow when Y_Z• is produced by NIR excitation. The uncompensated negative charge on the Mn cluster should decrease the reduction potential of Y_Z• and therefore increase the energy gap from P_{680}^+, which is the intermediate of the recombination reaction. Experiments in progress (C. Goussias and V. Petrouleas) reveal that the recombination rate of Y_Z• produced by NIR excitation of S_2 is strongly temperature dependent, and above ca. 35 K converges to that of the S_1Y_Z• intermediate, produced by visible-light excitation of S_1. Presumably, deprotonation of B_1 is thermally activated above 35 K. (iii) The intermediates decay preferentially by charge recombination of Y_Z• with Q_A^-, at liquid helium temperatures, while oxidation of the Mn cluster by Y_Z• is activated at elevated temperatures (*5*−*8*). The barriers associated with the transfer of the proton to and from base B_1 could explain this behavior but not in all cases. There should be no such barrier in the reoxidation of the manganese cluster by the NIR-induced Y_Z• radical. We may assume that the oxidation of the Mn cluster by tyrosine involves extra barriers associated with charge rearrangement, and/or changes in bond lengths. The NIR excitation gives the energy necessary to overcome these, but the reverse reaction requires thermal activation energy.

A Possible Molecular Model. It would be instructive to relate bases B and B_1 to known residues of the oxygen-evolving site. Base B could correspond to D1 His190 (D1 Tyr161). D1 Glu189, which according to the latest crystal structure at 3.2 Å resolution (*14*) appears to be equidistant from both the Mn cluster and TyrZ, could play the role of base B_1 (see also ref *28*). This latter choice should be examined in light of the mutation work on D1 Glu189 (*29*), which shows that five (Gln, Lys, Arg, Leu, and Ile) of 17 mutants examined sustain O_2 evolution at decreased levels (40−80% of the wild-type level). It is possible that some of the mutants can compensate for the B_1 function of Glu189 or certain steps of the mechanism are modified for the other mutants, resulting in both cases being less efficient. Actually, the fact that 12 mutants are incapable of O_2 evolution points to an important role of Glu189. To critically test the role of this residue, it would be very helpful if the low-temperature photochemistry of the mutants were studied in light of the considerations presented here. Scheme 4 illustrates the changes occurring during the S_1 to S_2 transition in correspondence to the first row of Scheme 2. Similar schemes can be produced for the other transitions and the various intermediates.

Implications for the Role of Tyr Z. These considerations suggest an intimate relationship between Tyr Z and the Mn cluster, but do not support the proposed role of Tyr Z as a H-atom abstractor (*4*). It is likely that the proton displacement toward base B during the oxidation of Tyr Z by P_{680}^+ could be the driving force for Mn deprotonation [role of Tyr Z as an electron abstractor and proton repeller (*7*, *8*)] particularly in the S_2 to S_3 (Scheme 3) and S_3 to S_4 transitions. This paper does not address the pathway of proton translocation, but an interesting proposal implicating Arg357 of CP43 can be found in ref *30*. It can also be noted that some of the constraints derived from these low-temperature data bear strong analogies to those in ref *30* based mostly on independent experimental evidence.

ACKNOWLEDGMENT

We are grateful to J. M. Mayer and B. A. Diner for insightful discussions.

REFERENCES

1. Goussias, C., Boussac, A., and Rutherford, A. W. (2002) Photosystem II and photosynthetic oxidation of water: An overview, *Philos. Trans. R. Soc. London, Ser. B 357*, 1369−1381.
2. Carrell, T. G., Tyryskin, A. M., and Dismukes, G. C. (2002) An evaluation of structural models for the photosynthetic water-oxidizing complex derived from spectroscopic and X-ray diffraction signatures, *J. Biol. Inorg. Chem. 7*, 2−22.
3. Diner, B. A., and Babcock, G. T. (1996) Structure, Dynamics, and Energy Conversion Efficiency in Photosystem II, in *Advances in Photosynthesis, Volume 4, Oxygenic Photosynthesis: the Light Reactions* (Ort, D. R., and Yocum, C. F., Eds.) Chapter 12, pp 213−247, Kluwer Academic Publishers, Dordrecht, The Netherlands.
4. Hoganson, C. W., and Babcock, G. T. (2000) Mechanistic Aspects of the Tyrosyl Radical-Manganese Complex in Photosynthetic Water Oxidation, in *Metals in Biological Systems* (Sigel, H., and Sigel, A., Eds.) Vol. 37, pp 613−656, Marcel Dekker, New York.
5. Nugent, J. H. A., Muhiuddin, I. P., and Evans, M. C. W. (2002) Electron transfer from the water oxidizing complex at cryogenic temperatures: The S_1 to S_2 step, *Biochemistry 41*, 4117−4126.
6. Ioannidis, N., and Petrouleas, V. (2002) Decay Products of the S_3 State of the Oxygen-Evolving Complex of Photosystem II at Cryogenic Temperatures. Pathways to the Formation of the $S = 7/2$ S_2 State Configuration, *Biochemistry 41*, 9580−9588.
7. Ioannidis, N., Nugent, J. H. A., and Petrouleas, V. (2002) Intermediates of the S_3 State of the Oxygen-Evolving Complex of Photosystem II, *Biochemistry 41*, 9589−9600.
8. Koulougliotis, D., Shen, J. R., Ioannidis, N., and Petrouleas, V. (2003) Near-IR irradiation of the S_2 state of the water oxidizing complex of photosystem II at liquid helium temperatures produces the metalloradical intermediate attributed to $S_1Y_Z^{\bullet}$, *Biochemistry 42*, 3045−3053.
9. Zhang, C., and Styring, S. (2003) Formation of split electron paramagnetic resonance signals in photosystem II suggests that tyrosine Z can be photooxidized at 5 K in the S_0 and S_1 states of the oxygen-evolving complex, *Biochemistry 42*, 8066−8076.
10. Nugent, J. H. A., Muhiuddin, I. P., and Evans, M. C. W. (2003) Effect of hydroxylamine on photosystem II: Reinvestigation of electron paramagnetic resonance characteristics reveals possible S state intermediates, *Biochemistry 42*, 5500−5507.
11. Peloquin, J. M., Campbell, K. A., and Britt, R. D. (1998) ^{55}Mn pulsed ENDOR demonstrates that the photosystem II "split" EPR signal arises from a magnetically-coupled mangano-tyrosyl complex, *J. Am. Chem. Soc. 120*, 6840−6841.
12. Dorlet, P., Di Valentin, M., Babcock, G. T., and McCracken, J. L. (1998) Interaction of $Y_Z^{\bullet}$ with its environment in acetate-treated photosystem II membranes and reaction center cores, *J. Phys. Chem. B 102*, 8239−8247.
13. Lakshmi, K. V., Eaton, S. S., Eaton, G. R., Frank, H. A., and Brudvig, G. W. (1998) Analysis of dipolar and exchange interactions between manganese and tyrosine Z in the $S_2Y_Z^{\bullet}$ state of acetate-inhibited photosystem II via EPR spectral simulations at X- and Q-Bands, *J. Phys. Chem. B 102*, 8327−8335.
14. Biesiadka, J., Loll, B., Kern, J., Irrgang, K.-D., and Zouni., A. (2004) Crystal structure of cyanobacterial photosystem II at 3.2 Å resolution: A closer look at the Mn-cluster, *Phys. Chem. Chem. Phys. 6*, 4733−4736.
15. Kamiya, N., and Shen, J. R. (2003) Crystal structure of oxygen-evolving photosystem II from *Thermosynechococcus vulcanus* at 3.7-Å resolution, *Proc. Natl. Acad. Sci. U.S.A. 100*, 98−103.
16. Ferreira, K. N., Iverson, T. M., Maghlaoui, K., Barber, J., and Iwata, S. (2004) Architecture of the photosynthetic oxygen-evolving center, *Science 303*, 1831−1838.
17. Faller, P., Pascal, A., and Rutherford, A. W. (2001) β-Carotene redox reactions in photosystem II: Electron-transfer pathway, *Biochemistry 40*, 6431−6440.
18. Sanakis, Y., Ioannidis, N., Sioros, G., and Petrouleas, V. (2001) A novel $S = 7/2$ configuration of the Mn cluster of photosystem II, *J. Am. Chem. Soc. 123*, 10766−10767.
19. Styring, S., and Rutherford, A. W. (1988) Deactivation kinetics and temperature dependence of the S-state transitions in the oxygen-evolving system of photosystem II measured by EPR spectroscopy, *Biochim. Biophys. Acta 933*, 378−387.
20. Zhang, C., Boussac, A., and Rutherford, A. W. (2004) Low-Temperature Electron Transfer in Photosystem II: A Tyrosyl Radical and Semiquinone Charge Pair, *Biochemistry 43*, 13787−13795.
21. Brettel, K., Schlodder, E., and Witt, H. T. (1984) Nanosecond reduction kinetics of photooxidized chlorophyll-a_{II} (P_{680}) in single flashes as a probe for the electron pathway, H^+-release and charge accumulation in the O_2-evolving complex, *Biochim. Biophys. Acta 766*, 403−415.
22. Diner, B. A. (2001) Amino acid residues involved in the coordination and assembly of the manganese cluster of photosystem II. Proton-coupled electron transport of the redox-active tyrosines and its relationship to water oxidation, *Biochim. Biophys. Acta 1503*, 147−163.
23. Rappaport, F., and Lavergne, J. (2001) Coupling of electron and proton transfer in the photosynthetic water oxidase, *Biochim. Biophys. Acta 1503*, 246−259.
24. Haumann, M., and Junge, W. (1996) Protons and Charge Indicators in Oxygen Evolution, in *Oxygenic Photosynthesis: The Light Reactions* (Ort, D. R., and Yocum, C. F., Eds.) pp 165−192, Kluwer Academic Publishers, Dordrecht, The Netherlands.
25. Nugent, J. H. A., Ball, R. J., and Evans, M. C. W. (2004) Photosynthetic water oxidation: The role of tyrosine radicals, *Biochim. Biophys. Acta 1655*, 217−221.
26. Faller, P., Rutherford, A. W., and Debus, R. J. (2002) Tyrosine D oxidation at cryogenic temperatures in photosystem II, *Biochemistry 41*, 12914−12920.
27. Vass, I., and Styring, S. (1991) pH-dependent charge equilibria between Tyr-D and the S states in photosystem II. Estimation of relative midpoint redox potentials, *Biochemistry 30*, 830−839.
28. Haumann, M., Mulkidjanian, A., and Junge, W. (1999) Tyrosine-Z in oxygen-evolving photosystem II: A hydrogen-bonded tyrosinate, *Biochemistry 38*, 1258−1267.
29. Debus, R. J., Campbell, K. A., Pham, D. P., Hays, A.-M. A., and Britt, R. D. (2000) Glutamate 189 of the D1 Polypeptide Modulates the Magnetic and Redox Properties of the Manganese Cluster and Tyrosine Y_Z in Photosystem II, *Biochemistry 39*, 6275−6287.
30. McEvoy, J. P., and Brudvig, G. W. (2004) Structure-based mechanism of photosynthetic water oxidation, *Phys. Chem. Chem. Phys. 6*, 4754−4763.

BI0503201